Michael Buchwitz on behalf of all co-authors 5-June-2018

Authors response to referee comments on manuscript "Computation and analysis of atmospheric carbon dioxide annual mean growth rates from satellite observations during 2003-2016" of Michael Buchwitz et al., MS No.: acp-2018-158

This document includes our point-by-point response to the reviews, a list of all relevant changes made in the manuscript, and a marked-up manuscript version.

Point-by-point response:

Our point-by-point response to the reviews has been submitted via the ACP website and is already online, see:

AC1: 'Reply to Anonymous Referee #1', Michael Buchwitz, 05 Jun 2018:

https://www.atmos-chem-phys-discuss.net/acp-2018-158/acp-2018-158-AC1-print.pdf

AC2: 'Reply to Anonymous Referee #2', Michael Buchwitz, 05 Jun 2018:

https://www.atmos-chem-phys-discuss.net/acp-2018-158/acp-2018-158-AC2-print.pdf

Nevertheless, these 2 documents with our answers are attached to this document (see following pages).

Marked-up manuscript version:

The Marked-up manuscript version is also attached to this document (at the end).

List of all relevant changes:

We have aimed at carefully addressing all referee comments (see our Point-by-point response). This resulted in several major and minor modifications, which have been implemented for the revised version of our manuscript (see Marked-up manuscript version). The most relevant changes are:

- Based on a comment from one of the referees we have slightly improved our method to compute the annual mean growth rates. This resulted in slight changes of most of the numerical values as listed in the paper (see marked-up manuscript version) and required to regenerate most of the figures. These modifications, however, did not led to any major modifications so that all general conclusions are still valid.
- We have added to few additional sentences to provide better explanations as requested by the referees.
- Furthermore, we have implemented some minor text modifications at various places.

We conclude that addressing the referee comments resulted in a significantly improved version of our manuscript. We hope that the revised version of the manuscript meets the high standards of ACP.

Michael Buchwitz on behalf of all co-authors

One the following pages please see

- our response to the two referees and
- the marked-up manuscript version.

Reply to Anonymous Referee #1

We thank the referee for carefully reading our manuscript and for providing the critical review. In the following, we provide answers to each of the referee's comments and concerns.

Addressing these comments, concerns and questions helped us to prepare a significantly improved version of our manuscript.

General comments

C1: Referee:
The paper describes the analysis of column-average dry-air mole fractions of CO2 observed by SCIAMACHY and GOSAT. The data being analysed represent over a decade of substantial international efforts and is an amazing accomplishment that is documented in many previous papers. The headline figures from this paper look impressive but the subsequent analysis is weak and does not add much to the main paper. Below I substantiate these comments. I recommend the paper be published but only after the major issues are addressed.

Author's reply:
The primary objectives of the paper are

(i) to present a new global data set, which has not yet been published in a peer-reviewed journal,
(ii) to describe and apply a method to compute annual mean growth rates from this data set and
(iii) to interpret the variations of the derived annual mean growth rates.

The analysis of the annual CO_2 growth rates can be extended and enhanced e.g., by using appropriate and comprehensive modelling and considering additional data sets. However, we consider that our analysis is a relevant and important approach, which is independent of atmospheric model assumptions and uses available time series of data. Below we explain how we plan to address the major and minor comments as given in the review in order to improve the paper.

Major points

C2: Referee:
The authors will be acutely aware that it is difficult to compare NOAA ground-based data with XCO2 data from ground-based or space-based remote sensing instruments. Columns are an integrated sum of many geographically distributed sources and sinks from a range of times that have been distributed throughout the atmosphere. Consequently, it is difficult to compare NOAA and XCO2 CO2 growth rates. Here, I am suggesting only that the authors acknowledge this as a difficulty.

Author's reply:

We agree that annual growth rates of CO_2 determined from the NOAA in situ ground based measurements, which are very accurate but sparsely distributed, will not necessarily be identical with the annual growth rates computed from measurements of the dry column atmospheric mixing ratios or mole fractions of CO_2 measured over cloud free scenes from space.

Atmospheric CO_2 has different sources and sinks. Changes in the biological sources of CO_2, such as respiration and bacterially initiated decomposition and oxidation of organic matter, contribute significantly to changes of the CO_2 growth rate. Furthermore, CO_2 has a variety of geologic sources such as volcanic eruptions. Changes of the amount of CO_2 from volcanic eruption may contribute to the mean annual CO_2 growth rate. A small amount of CO2 is produced by the oxidation of CO initiated by OH. CO_2 is removed from the atmosphere by the biosphere through photosynthesis on the land and in the ocean. This accounts for the removal of around half of the CO_2 emitted each year. As is well known, CO_2 is only significantly removed chemically or photochemically at high altitude from the atmosphere by the reactions of O(1D), its short wave UV photolysis and ion-molecule reactions. In the mesosphere and thermosphere, the column of CO_2 is only a small component of the total column. For chemically long lived gases such as CO_2 differences in atmospheric ratio at any point in the atmosphere depends on the time taken for CO2 to mix. After its release or removal, which takes place primarily at the surface or in the boundary layer, the air mass with elevated or depleted CO_2 is transported by advection and convection and mixes into the atmosphere. This impacts on the horizontal and vertical distributions of CO_2. The reduction of CO_2 as a function of altitude enables the age of air mass to be estimated in the stratosphere, where vertical mixing is slow and varies in the range 2-8 years. In the troposphere mixing times are faster than exchange between the troposphere

and the stratosphere. It therefore cannot be expected that annual mean growth rates computed from CO_2 measurements at the surface are exactly identical with growth rates computed from XCO_2.

Nevertheless, growth-rates from NOAA are the de facto standard and therefore we think that it is very important to show comparisons with this reference data set.

In order to better acknowledge this difficulty we will add the following sentence at the end of the paragraph, where the comparison with the NOAA growth rates is presented: "Perfect agreement is not to be expected as these two growth rate time series have been obtained from CO_2 observations, which represent very different vertical sampling of the atmosphere (surface (NOAA) versus entire vertical column (satellite))".

C3: Referee:
The global growth rates determined by XCO2 are I believe valid and physically meaningful. However, regional growth rates (no matter how you divide the Earth) make little or no sense because of atmospheric transport that moves air from one region (e.g. zonal band indicative of midlatitudes) to another. It is tempting to interpret regional growth rates, but they are (strictly speaking) scientifically meaningless without understanding changes in atmospheric transport. By (implicitly) ignoring atmospheric transport the authors are essentially assuming that observed regional CO2 variations results exclusively from that region.

Author's reply:
We are aware of the fact that atmospheric transport cannot be ignored in this context. In our manuscript, we have not aimed at interpreting regional growth rates in terms of regional changes. In fact, we expect the growth rates to be not exactly identical but similar (taking into account the uncertainty of our growth rate) due to atmospheric transport and mixing. Therefore, we write: "Growth rate time series for several latitude bands are shown in Fig. 4. As can be seen from Fig. 4, the growth rates are similar in all latitude bands including the global results (for numerical values see Tab. 2). The reason for this is that atmospheric CO2 is long-lived and therefore well-mixed." The only figure where we aim at interpretation in terms of emissions and ENSO is Fig. 5 and here we only use the derived global growth rates. Because we use a XCO2 data set that is spatially resolved, we think that it is important to compute and discuss growth rates determined not only from globally averaged XCO2 but also from regionally averaged XCO2. This is important as this tells us something about the quality of the satellite data set and of the derived growth rates especially if one assumes that growth rates are expected to be similar for the selected regions.

To make the above argument clearer in the manuscript, we will add the following sentences in the paragraph, where we discuss Fig. 4:
"As a result of atmospheric transport and mixing, similar mean annual CO_2 growth rates, within their measurements error, are expected for all values derived at the different latitude bands. This behaviour is shown in Fig. 4 and is interpreted as an indication of the good quality of the satellite XCO_2 data product and the adequacy of the method used to compute the annual mean CO_2 growth rates."

C4: Referee:
The authors' attempt at quantifying the respective role of human emissions and ENSO on CO2 growth rates is unfortunately (at least in this reviewer's opinion) a fool's errand. Our knowledge of human emissions is relatively good but still poor. Liu et al 2017 (Science) showed contrasting tropical carbon cycle responses in response to ENSO. These different responses will only complicate the correlative analysis of CO2 growth rate and ENSO indices.

Author's reply:
Our approach to quantify the different roles is based on our new growth rate time series and well-established other time series. Our estimation method to quantify contributions from human emissions and ENSO is one attempt to address this aspect but we do not claim that our approach is the best possible. We think however that our approach is at least a reasonable and an important first step and we aimed at presenting our method as clearly as possible so that readers can judge to what extent they find the corresponding result useful or not.

We do not consider the task of trying to separate the impact of human emissions and that of ENSO on the mean annual CO_2 growth rate is a fool's errand. Rather we consider our approach is an example of an Occam's razor i.e. in explaining a thing (here: the variation of the satellite-derived growth rate), no more assumptions should be made than are necessary. Nevertheless, we agree that our growth rates may contain more information than extracted using the method applied in our paper.

The interesting work of Liu et al 2017 (Science) uses a complex earth model, constrained by a limited number of satellite observations in the tropics and other a priori knowledge, to identify different responses in the different tropical continents to the surface flux of CO_2 and thus carbon. Our approach to quantify the different roles of ENSO and anthropogenic fossil fuel emissions uses the reported time series of mean annual CO_2 growth rates and well-established time series of ENSO indices and the known estimates of anthropogenic emissions from fossil fuel combustion and industry. This approach is our attempt to address what we and others consider an important issue viz: the attribution of growth rate variations to known anthropogenic emissions from fossil fuel combustion and industry and to that from the impact of ENSO. The latter has many potential impacts on the earth system amongst which are in the tropics the creation of regions of flooding and drought, increasing fire and biomass burning and changing sea surface temperature. These effects all impact on the growth rate of CO_2 in different ways. However, in this study we have not tried to separate the different impacts of ENSO. Rather in this study, we attribute the importance of ENSO and the known anthropogenic fossil fuel combustion and industry sources to the observed annual growth rates. Our results are not in conflict with this scientific finding of Liu et al 2017 (Science). The use of our longer term time series of XCO_2 provides an opportunity when coupled with models to investigate the regional impacts of ENSO both in the tropics and the extra tropics in a separate study.

Overall, we consider that our approach is relevant, reasonable and plausible. We describe our assumptions and the derivation of the attribution clearly so that readers can reproduce the results, criticise our assumptions and make improved analyses.

Minor points

C5: Referee:
Line 6. Geological processes are only a minor sink of CO2 over decadal scales. I applaud the authors being comprehensive but this reviewer suggests a focus on the timescales that correspond to the analysis being presented.

Author's reply:
For the revised version of the manuscript we will remove the link to geological processes in the introduction.

C6: Referee:
Line 10/11. Relating GtC/yr to ppm is an undergraduate exercise that barely needs a reference let alone two.

Author's reply:
We will remove one of the two references keeping only the reference to Ballantyne et al., 2012.

Reply to Anonymous Referee #2

We thank the referee for carefully reading our manuscript and for providing a critical review. Below we provide point-by-point answers to each of the referee's comments and concerns. Addressing these comments, concerns and questions helped us to prepare a significantly improved version of our manuscript.

General comments

C1: Referee:
This manuscripts computes the CO2 growth rate from a combination of two near infrared satellite sensors over almost a decade and a half. The authors show that their estimated growth rates are in line with NOAA growth rates computed from marine boundary layer sites, and variations in the growth rate are correlated with expected mechanisms such as the ENSO cycle and anthropogenic emissions. This is all reasonable. However, I do not think that Atmospheric Chemistry and Physics is the correct journal for publishing this manuscript, because the manuscript does not present anything new about either the atmosphere or surface processes that influence the atmosphere (my comments on variation partitioning follow later). What I learned from this manuscript is that the merged XCO2 data product Obs4MIPs gives global CO2 growth rates that are reasonable, in line with other estimates, and can be correlated with known factors influencing the carbon budget. This is a perfectly fine message, but it's primarily a message about the Obs4MIPs data product, and therefore a better venue for it would be an alternative measurement- or data-focused journal such as Atmospheric Measurement Techniques or Earth System Science Data. If the authors insist on publishing this in ACP and the editor agrees, I would strongly suggest making this a technical note instead of a research article.

Author's reply:
We agree that the manuscript would also be appropriate for a measurement- or data-focused journal and in fact we carefully thought about this option before submission to ACP. We finally concluded that ACP is appropriate because the interpretation of the satellite-derived XCO2 data set is a focus of the manuscript.

We do not consider that our manuscript is simply a technical note. It is true that the data set and the presented analysis does not show obvious contradictions with current knowledge. However, the evidence base for current knowledge is limited to the sparse but accurate ground based measurements of the in situ mixing ratios. We present an independent data set of the dry column CO_2 mixing ratio or mole fraction, XCO2, and the first derived annual mean growth CO_2 rates using this XCO2 data set. The values are similar to those derived from the ground based in situ mixing ratio measurements. The novel nature of our manuscript is that we present

(i) a new global XCO2 data set covering more than a decade,
(ii) a method to compute annual mean growth rates from this data set,
(iii) a comparison with NOAA (de facto standard) growth rates, which agrees well and thereby validates both approaches and
(iv) an interpretation of the derived growth rates to compare the impact of ENSO on the mean annual CO2 growth rate with that from fossil fuel combustion and industry.

The analysis of XCO2 and the derived annual growth rates can be enhanced and extended, e.g., by using appropriate and probably very comprehensive modelling and considering additional data sets. This would enable regional surface fluxes to be assessed. However, we consider this as outside of the scope of the current manuscript. Nevertheless, we consider our analysis as an important step in terms of interpreting the satellite-derived growth rates. It provides independent and global knowledge about the annual mean CO_2 growth rate.

Our preferred option would be to publish this paper in ACP (as also supported by the other referee) but of course, it is up to the Editor to decide.

C2: Referee:
Regardless of where this manuscript is published, there are a few issues that I would recommend the authors address, which are as follows:

(1) I fail to see the significance of splitting the growth rate into latitude bands. The authors must be well aware that such a split, while numerically possible, is impossible to tie to any set of surface processes because of atmospheric mixing, since the interhemispheric mixing time is a year or less. What was the authors' purpose behind deriving growth rates in zonal bands?

Author's reply:

One motivation of the approach taken was to assess the quality of the satellite XCO2 data product and of the method developed to compute annual mean growth rates. We are aware of the fact that atmospheric transport cannot be ignored and that transport and mixing will result in similar growth rates (compared to our uncertainty) for different latitude bands. We expect the latitudinal annual CO2 growth rates and the global CO2 annual growth rates to be very similar, which is what we find. Therefore, we write: "Growth rate time series for several latitude bands are shown in Fig. 4. As can be seen from Fig. 4, the growth rates are similar in all latitude bands including the global results (for numerical values see Tab. 2). The reason for this is that atmospheric CO2 is long-lived and therefore well-mixed."

In our manuscript, we have not aimed at interpreting regional growth rates in terms of regional changes. The only figure where we aim at interpretation in terms of emissions and ENSO is Fig. 5 and here we only use the derived global growth rate. Because we use a XCO2 data set that is spatially resolved, we think that it is important to compute and discuss growth rates determined not only from globally averaged XCO2 but also from regionally averaged XCO2. This is important as this tells us something about the quality of the satellite data set and of the method used to compute growth rates. If there is a good reason, why the growth rates should be similar for all regions (see above) and if the satellite data set would not show this, then this would indicate that the satellite data or the method usedf to compute growth rates from these data would suffer from a potentially serious problem. We therefore think that it is important to compute and discuss not only growth rates computed from the global data set but also from regional sub-sets. To make this clearer we will add the following text in the paragraph, where we discuss Fig. 4:

"As a result of atmospheric transport and mixing, similar mean annual CO2 growth rates, within their measurements error, are expected for all values derived at the different latitude bands. This behaviour is shown in Fig. 4 and is interpreted as an indication of the good quality of the satellite XCO2 data product and the adequacy of the method used to compute the annual mean CO2 growth rates."

C3: Referee:
(2) While computing the global average XCO2, did the authors account for differing surface areas at different latitudes? There is less atmospheric mass at high latitudes, and unless this is taken into account, a straight-up averaging of gridded XCO2 globally is not going to give the correct mean CO2 mole fraction, which would invalidate its link with the global flux. It's not clear from the manuscript if the authors already took care of this (the NOAA estimate includes proper weighting by surface area [Ballantyne et al, 2012]).

Author's reply:
For the revised version of the manuscript, we have improved the description of our method taking the referee's comment into account. Instead of unweighted averaging, we will compute monthly XCO2 values for global or regional averages by weighting with the latitude dependent area, i.e., by weighting with the cosine of latitude. To explain this we will add these sentences: "To compute the spatially averaged XCO2 time series (shown in Fig. 2a), we first longitudinally average the XCO2 followed by the computation of the area-weighted latitudinal average of XCO2 by using the cosine of latitude as weight. We consider surface area because surface fluxes are linked to mass of CO2 (or number of CO2 molecules) rather than molecular mixing ratios or mole fractions.". Our analysis shows that this leads to minor changes of most of the numbers, figures and tables presented in our initial manuscript but it will not affect any major conclusion.

C4: Referee:
(3) Every El Niño is different. Some cause large changes in ocean fluxes, while others cause large changes in land fluxes, which in turn can either be ecosystem-driven or fire-driven [Sarmiento et al, 2010]. The growth rate in global CO2 is a combination of all possible factors. To try and correlate this growth rate with an ocean-only indicator like ONI or SOI is a drastic oversimplification. To then use that correlation to infer the percentage variation in the growth rate due to ENSO (as opposed to fossil fuel emissions) is even less robust. If the authors really want to dig into the factors behind CO2 variability, I would suggest some index more strongly tied to the terrestrial biosphere, such as biomass-weighted precipitation or temperature anomalies, which in turn are influenced by ENSO.

Author's reply:
We agree that the relationship between atmospheric CO2 growth rate variations and underlying source/sink related processes is a very complex one. We would like to contribute to a much better understanding of these links but we acknowledge that our manuscript is very limited in this respect. We have used ONI and SOI as proxies for ENSO and ENSO-related effects because these are well-established indices. Our objective was to compare the impact of

ENSO on the annual mean growth rate as compared to that of the emission from fossil fuel combustion and industry. This goal we have achieved. More detailed analysis of the impact of the individual ENSO cycles on the biosphere and the land requires comparison with complex earth system models.

C5: Referee:
(4) SCIAMACHY sensors were degraded a few years into flight, influencing the precision of retrieved XCH4 [Frankenberg et al, 2011]. Was a similar effect seen for retrieved XCO2? If so, why doesn't that should up as larger errors bars in figure 3(c) after 2006?

Author's reply:
SCIAMACHY XCH4 is retrieved from a different spectral region than XCO2. The spectral region beyond 1.6 microns in SCIAMACHY used Ge doped InGaAs detectors. These detectors were more sensitive to high energy proton bombardment. Individual detector pixels after being impacted by a high energy proton had increased noise. This effect indeed made the XCH4 error larger but the XCO2 data product is not impacted by this effect.

References:

[1] A. P. Ballantyne, C. B. Alden, J. B. Miller, P. P. Tans, and J. W. C. White, "Increase in observed net carbon dioxide uptake by land and oceans during the past 50 years," Nature, vol. 488, no. 7409, pp. 70–72, Aug. 2012.

[2] C. Frankenberg, I. Aben, P. Bergamaschi, E. J. Dlugokencky, R. van Hees, S. Houweling, P. van der Meer, R. Snel, and P. Tol, "Global column-averaged methane mixing ratios from 2003 to 2009 as derived from SCIAMACHY: Trends and variability," J. Geophys. Res., vol. 116, no. D4, p. D04302, Feb. 2011.

[3] J. L. Sarmiento, M. Gloor, N. Gruber, C. Beaulieu, A. R. Jacobson, S. E. M. Fletcher, S. Pacala, and K. Rodgers, "Trends and regional distributions of land and ocean carbon sinks," Biogeosciences, vol. 7, no. 8, pp. 2351–2367, 2010.

The following pages show the

marked-up manuscript version

Computation and analysis of atmospheric carbon dioxide annual mean growth rates from satellite observations during 2003-2016

Michael Buchwitz[1], Maximilian Reuter[1], Oliver Schneising[1], Stefan Noël[1], Bettina Gier[1,2], Heinrich Bovensmann[1], John P. Burrows[1], Hartmut Boesch[3,4], Jasdeep Anand[3,4], Robert J. Parker[3,4], Peter Somkuti[3,4], Rob G. Detmers[5], Otto P. Hasekamp[5], Ilse Aben[5], André Butz[2,6], Akihiko Kuze[7], Hiroshi Suto[7], Yukio Yoshida[8], David Crisp[9], Christopher O'Dell[10]

[1]Institute of Environmental Physics (IUP), University of Bremen, Bremen, Germany

[2]Deutsches Zentrum für Luft- und Raumfahrt e.V. (DLR), Institut für Physik der Atmosphäre, Oberpfaffenhofen, Germany

[3]Earth Observation Science, University of Leicester, Leicester, UK

[4]NERC National Centre for Earth Observation, Leicester, UK

[5]SRON Netherlands Institute for Space Research, Utrecht, The Netherlands

[6]Meteorologisches Institut, Ludwig-Maximilians-Universität (LMU), Munich, Germany

[7]Japan Aerospace Exploration Agency (JAXA), Tsukuba, Japan

[8]National Institute for Environmental Studies (NIES), Tsukuba, Japan

[9]Jet Propulsion Laboratory (JPL), Pasadena, CA, USA

[10]Colorado State University (CSU), Fort Collins, CO, USA

Correspondence to: Michael Buchwitz (Michael.Buchwitz@iup.physik.uni-bremen.de)

Abstract. The growth rate of atmospheric carbon dioxide (CO_2) reflects the net effect of emissions and uptake resulting from anthropogenic and natural carbon sources and sinks. Annual mean CO_2 growth rates have been determined globally and for selected latitude bands from satellite retrievals of column-average dry-air mole fractions of CO_2, i.e., XCO_2, for the years 2003 to 2016. The global XCO_2 growth rates agree with National Oceanic and Atmospheric Administration (NOAA) growth rates from CO_2 surface observations within the uncertainty of the satellite-derived growth rates (mean difference ± standard deviation: 0.0±0.3 ppm/year; R: 0.82). This new and independent data set confirms record large growth rates around 3 ppm/year in 2015 and 2016, which are attributed to the 2015/2016 El Niño. Based on a comparison of the satellite-derived growth rates with human CO_2 emissions from fossil fuel combustion and with El Niño Southern Oscillation (ENSO) indices, we estimate by how much the impact of ENSO dominates the impact of fossil fuel burning related emissions in explaining the variance of the atmospheric CO_2 growth rate.

Gelöscht: Institute of Atmospheric Physics, Deutsches Zentrum für Luft- und Raumfahrt (DLR), Oberpfaffenhofen, Germany

Gelöscht: 24

Gelöscht: 7

1 Introduction

Atmospheric carbon dioxide (CO_2) is an important greenhouse gas that causes global warming (IPCC 2013). Sources that emit CO_2 into the atmosphere include anthropogenic and natural sources at the surface, and the oxidation of carbon monoxide and hydrocarbons in the atmosphere. The sinks that remove CO_2 primarily at the surface include biological (photosynthesis) and physical (solubility) processes. Anthropogenic emissions of CO_2, primarily from fossil fuel combustion, have increased the atmospheric CO_2 mixing ratios at the surface by more than 40% since pre-industrial times, from less than 280 parts per million (ppm) to 402.8±0.1 ppm in 2016 (Dlugokencky and Tans, 2017a). A global increase of atmospheric CO_2 by 1 ppm in a one-year time period corresponds to an annual increase of 2.12 GtC/year (Ballantyne et al., 2012). However, this increase in mass does not directly correspond to the emissions. The reason is that only a fraction of the emitted CO_2 remains in the atmosphere as CO_2 is partitioned between the atmosphere and ocean and land carbon sinks. On average, somewhat less than half of the emitted CO_2 remains in the atmosphere but this "airborne fraction" varies substantially from year to year (Le Quéré et al., 2016, 2018). Variations of the airborne fraction are not well understood primarily because of an inadequate understanding of the terrestrial carbon sink, which introduces large uncertainties for climate prediction (e.g., IPCC 2013; Peylin et al., 2013; Wieder et al., 2015; Huntzinger et al., 2017). Identification of the origin of changes of the growth rate requires additional information for the attribution to particular sources or sinks (Peters et al., 2017). Atmospheric CO_2 growth rates inferred from in-situ CO_2 surface measurements are regularly determined and published, for example, by the National Oceanic and Atmospheric Administration (NOAA) (see https://www.esrl.noaa.gov/gmd/ccgg/trends/gr.html). In this study, we present and interpret atmospheric growth rates determined from the remote sensing of CO_2 vertical columns from space, which are described in the following section.

Gelöscht: ,

Gelöscht: and some geologic

Gelöscht: (e.g., carbonate weathering)

Gelöscht: ; Prather et al., 2012

Gelöscht: 7

2 Global satellite observations of atmospheric CO_2 columns

Satellites provide retrievals of CO_2 vertical columns in terms of the CO_2 column-average dry-air mole fraction, denoted XCO_2. Although a relatively new field, satellite-based XCO_2 data products have already been used to improve our knowledge of natural (e.g., Basu et al., 2013; Maksyutov et al., 2013; Chevallier et al., 2014; Reuter et al., 2014a; Schneising et al., 2014; Houweling et al., 2014; Parker et al., 2016; Heymann et al., 2017; Liu et al., 2017; Kaminski et al., 2017) and anthropogenic (e.g., Schneising et al., 2013; Reuter et al., 2014b; Kort et al., 2012; Hakkarainen et al., 2016; Nassar et al., 2017) CO_2 sources and sinks but only a few studies explicitly present and discuss CO_2 growth rates. Buchwitz et al., 2007, analyzed the first three years (2003-2005) of XCO_2 retrievals from SCIAMACHY/ENVISAT (Burrows et al., 1995; Bovensmann et al., 1999) generated using the WFM-DOAS retrieval algorithm (Buchwitz et al., 2006). They computed year-to-year CO_2 variations and compared the XCO_2 increase with the XCO_2 increase computed from the output of NOAA's CO_2 assimilating system CarbonTracker (Peters et al., 2007) and found agreement within 1 ppm/year. Schneising et al., 2014, computed growth rates from the 2003-2011 SCIAMACHY XCO_2 record. They compared the derived annual growth rates with surface temperature and found that years having higher temperatures during the vegetation growing season are associated with larger growth rates in atmospheric CO_2 at northern mid-latitudes. Growth

rates from GOSAT (Kuze et al., 2016) are published by the National Institute for Environmental Studies (NIES), Tsukuba, Japan (NIES 2017).

In this study, we analyze a new satellite XCO_2 data set covering 14 years (2003-2016) generated from SCIAMACHY/ENVISAT and TANSO-FTS/GOSAT. We use the XCO_2 data product Obs4MIPs (Observations for Model Intercomparisons Project) version 3 (O4Mv3), which is a gridded (Level 3) monthly data product at 5^o latitude by 5^o longitude spatial resolution in Obs4MIPs format (Buchwitz et al., 2017a). Obs4MIPs (https://www.earthsystemcog.org/projects/obs4mips/) is an activity to make observational products more accessible for climate model intercomparisons (e.g., Lauer et al., 2017). The O4Mv3 XCO_2 data product was generated by gridding (averaging) the XCO_2 Level 2 (i.e., individual soundings) product generated with the Ensemble Median Algorithm (EMMA, Reuter et al., 2013). EMMA uses as input an ensemble of XCO_2 Level 2 data products (Buchwitz et al., 2015, 2017a, 2017b; Reuter et al., 2013) from SCIAMACHY/ENVISAT and TANSO-FTS/GOSAT. To generate the O4Mv3 product, the EMMA version 3.0 (EMMAv3, Reuter et al., 2017e) product was used. The list of satellite products used for the generation of the EMMAv3 Level 2 product - and therefore also for the O4Mv3 Level 3 data product used in this study - is provided in Tab. 1. The quality of this product relative to Total Carbon Column Observing Network (TCCON) ground-based observations (Wunch et al., 2011, 2015) can be summarized as follows (Buchwitz et al., 2017c): +0.23 ppm overall (global) bias, relative accuracy 0.3 ppm (1-sigma), and very good stability in terms of linear bias trend (-0.02±0.04 ppm/year).

Figure 1 presents an overview of the O4Mv3 product in terms of time series and global XCO_2 maps. The maps show the typical coverage of XCO_2 from SCIAMACHY (until April 2012) and GOSAT (since mid 2009). As can be seen, the time series for the three latitude bands shown in Fig. 1 have very similar slopes. They mainly differ in the amplitude of the seasonal cycle, which reflects the latitudinal dependence of uptake and release of atmospheric CO_2 by the terrestrial biosphere (Schneising et al., 2014). These time series have been used to compute annual mean CO_2 growth rates as will be explained in the following section.

3 Atmospheric CO_2 growth rates from satellite observations

National Oceanic and Atmospheric Administration (NOAA) defines the annual mean CO_2 growth rate for a given year as the CO_2 concentration difference at the end of that year minus the CO_2 concentration at the beginning of that year (Thoning et al., 1989; see also additional explanations as given on the NOAA/ESRL website (https://www.esrl.noaa.gov/gmd/ccgg/about/global_means.html)). We adopt this definition. As described below, our method involves the following three steps: (i) Computation of an XCO_2 time series (at monthly resolution and sampling) by averaging the XCO_2 in the region of interest. (ii) Computation of monthly sampled XCO_2 annual growth rates by computing the difference of the XCO_2 value of month i minus the XCO_2 value of month i-12 and computation of the corresponding uncertainty estimate. (iii) Computation of annual mean growth rates and their corresponding uncertainties from the monthly sampled annual growth rates.

In the following, this method is described in detail using Fig. 2 for illustration. Figure 2 shows how the growth rates are computed for the latitude band 30^oN-60^oN, i.e., for northern mid-latitudes. In Figure 2a monthly satellite XCO_2 (O4Mv3), as obtained by averaging all the individual (5^ox5^o) XCO_2 values in the selected latitude band, is

plotted. To compute the spatially averaged XCO_2 time series (shown in Fig. 2a), we first longitudinally average the XCO_2 followed by the computation of the area-weighted latitudinal average of XCO_2 by using the cosine of latitude as weight. We consider surface area because surface fluxes are linked to mass of CO_2 (or number of CO_2 molecules) rather than molecular mixing ratios or mole fractions. As can be seen, the computed time series does not start at the beginning of 2003 but in April 2003. As explained in Buchwitz et al., 2017d (see discussion of their Fig. 6.1.1.1) the underlying SCIAMACHY BESD v02.01.02 XCO_2 data product (see Tab. 1) apparently suffers from an approximately 1 ppm high bias in the first few months of 2003. The exact magnitude of this bias has not been quantified due to lack of TCCON validation data in this early time period. As this bias in early 2003 is critical for the year 2003 growth rate, we have omitted the first three months of 2003 for the computation of the growth rates shown in this publication.

Formatiert: Tiefgestellt
Formatiert: Tiefgestellt
Formatiert: Tiefgestellt
Formatiert: Tiefgestellt
Formatiert: Tiefgestellt

Figure 2b shows monthly sampled annual growth rates as computed from the monthly XCO_2 values shown in Fig. 2a. Each value is the difference of two monthly XCO_2 values corresponding to the same month (e.g., January) but different years (e.g., 2004 and 2005). For example, the first data point (first diamond symbol) shown in Fig. 2b is the difference of the April 2004 XCO_2 value minus the April 2003 XCO_2 value. The second data point corresponds to May 2004 minus May 2003, etc. The time difference between the monthly XCO_2 pairs is always one year and the time assigned to each XCO_2 difference is the time in the middle of that year. Therefore, the time series shown in Fig. 2b starts six months later and ends six months earlier as compared to the time series shown in Fig. 2a. Each XCO_2 difference shown in Fig. 2b therefore corresponds to an estimate of the XCO_2 annual growth rate and the position on the time-axis corresponds to the middle of the corresponding one-year time period.

A 1-sigma uncertainty estimate has been computed for each of the monthly sampled annual growth rates shown in Fig. 2b (see grey vertical bars). They have been computed such that they reflect the following aspects: (i) the standard error of the O4Mv3 XCO_2 values as given in the O4Mv3 data product file for each of the 5^ox5^o grid cells, (ii) the spatial variability of the XCO_2 within the selected region, (iii) the temporal variability of the annual growth rates in the one year time interval, which corresponds to the annual growth rate, and (iv) the number of months (N) with data located in that one year time interval. The uncertainties have been computed as the mean value of three terms divided by the square root of N. The first term is the mean value of the standard error, the second term is the standard deviation of the XCO_2 values in the selected region and the third term is the standard deviation of the monthly sampled annual growth rates in the corresponding one-year time interval.

Figure 2c shows the final result, i.e., the annual mean XCO_2 growth rates and their estimated (1-sigma) uncertainties. The annual mean growth rates have been computed by averaging all the monthly sampled annual growth rates (shown in Fig. 2b), which are located in the year of interest (e.g., 2003). For most years, 12 annual growth rate values are available for averaging but there are some exceptions. For example, for the year 2003 only 3 values are present as can be seen from Fig. 2b and for the years 2014 and 2015 there are only 11 values as no data are available for January 2015 due to issues with the GOSAT satellite. The uncertainty of the annual mean growth rate has been computed by averaging the uncertainties assigned to each of the monthly sampled annual growth rates (shown as grey vertical bars in Fig. 2b) scaled with a factor, which depends on the number of months (N) available for averaging. This factor is the square root of 12/N. It ensures that the uncertainty is larger,

the less data points are available for averaging. Overall, our uncertainty estimate is quite conservative, as we do not assume that errors improve upon averaging. As a result of this procedure, the error bar of the year 2003 growth rate is quite large (0.72 ppm/year, see Tab. 2, where all numerical values are listed). This is because the monthly sampled annual growth rate varies significantly in 2003 (see Fig. 2b) and because only N=3 data points are available for averaging in 2003. In contrast, the year 2005 growth rate uncertainty is much smaller (0.26 ppm/year) because the growth rates vary only little during 2005 and because N=12 data points are available for averaging.

Figure 3 shows the corresponding results for the global data set. As can be seen, all time series are similar to the ones shown in Fig. 2 for northern mid-latitudes. However, there are also difference, e.g., the seasonal cycles as shown in Fig. 2a and Fig. 3a. For northern mid-latitudes (Fig. 2a) the shape of these cycles is very similar for all years in contrast to the global data shown in Fig. 3a. This is due to spatial sampling differences as the first few years (until 2008) are "land only" data as the SCIAMACHY XCO_2 is limited to observations over land whereas GOSAT XCO_2 (from 2009 onwards) is not restricted to land (see global maps shown in Fig. 1). For the northern mid-latitude region the land coverage dominates (see global map in Fig. 2a). Therefore, for northern mid-latitudes SCIAMACHY and GOSAT sample similar regions, in contrast to the global region (Fig. 3), where the spatial sampling differences are larger. In Fig. 3c also the NOAA global growth rates (Dlugokencky and Tans, 2017b) are shown. As can be seen, the satellite-derived growth rates agree well with the NOAA growth rates obtained from CO_2 surface observations. For the time period 2003-2016 the linear correlation coefficient R is 0.82 and the difference is -0.02±0.28 ppm/year (mean difference ± standard deviation). Perfect agreement is not to be expected as these two growth rate time series have been obtained from CO_2 observations, which represent very different vertical sampling of the atmosphere (surface (NOAA) versus entire vertical column (satellite)).

Growth rate time series for several latitude bands are shown in Fig. 4. As can be seen from Fig. 4, the growth rates are similar in all latitude bands including the global results (for numerical values see Tab. 2). The reason for this is that atmospheric CO_2 is long-lived and therefore well-mixed. As a result of atmospheric transport and mixing, similar mean annual CO_2 growth rates, within their measurements error, are expected for all values derived at the different latitude bands. This behaviour is shown in Fig. 4 and is interpreted as an indication of the good quality of the satellite XCO_2 data product and the adequacy of the method used to compute the annual mean CO_2 growth rates. As can also be seen from Fig. 4, the largest growth rates are approximately 3 ppm/year during 2015 and 2016. These record large growth rates (Peters et al., 2017) are attributed to the consequences of the strong 2015/2016 El Niño event, which produced large CO_2 emissions from fires and enhanced net biospheric respiration in the tropics relative to normal conditions (Heymann et al., 2017; Liu et al., 2017). Many of these fires are initiated by humans, for example, to clear tropical forests. In this study, human emissions of CO_2 are defined as emissions from fossil fuel combustion and industry (Le Quéré et al., 2016, 2018) but do not include, for example, CO_2 emissions originating from slash and burn agriculture.

4 Correlation of CO_2 growth rates with fossil CO_2 emissions and ENSO indices

Figure 5 shows a comparison of the CO_2 annual mean growth rates (Fig. 5a) with annual global CO_2 emissions from fossil fuel combustion and industry (Fig. 5b) (Le Quéré et al., 2018; GCP 2017) (correlation of growth rate

Gelöscht: 69

Gelöscht: 5

Gelöscht: 7

Gelöscht: 4

Formatiert: Tiefgestellt

Formatiert: Nicht Hervorheben

Gelöscht: 7

Gelöscht: 7

and human emissions: R^2 = 31%). As can be seen, the growth rates vary significantly in recent years despite nearly constant human emissions. Figure 5d shows two ENSO indices: the Southern Oscillation Index (SOI, blue lines) (NOAA 2017a; Ropelewski and Jones, 1987) and the Oceanic Niño Index (ONI, green lines) (NOAA 2017b). Whereas SOI is defined as the normalized pressure difference between Tahiti and Darwin (values less than -1 indicate the presence of a strong El Niño), ONI is based on Sea Surface Temperature (SST) differences (positive values correspond to El Niño). The dotted lines correspond to the original (i.e., unshifted) annual mean indices and the solid lines correspond to time shifted ENSO indices. Time shifts have been investigated to consider the delay in atmospheric response to ENSO-induced changes. As shown in Fig. 5c, the growth rate response as quantified by R^2 is largest after 4 months for ONI (R^2 = 35%) and after 7 months for SOI (R^2 = 30%). These maxima have been adopted for the solid (shifted) lines in Fig 5d. This finding is consistent with results from other studies, where lags in the range 3-9 months have been reported (Jones et al., 2001; Chylek et al., 2018).

In order to quantify the impact of the human CO_2 emissions and of ENSO, as described by the two indices SOI and ONI, on growth rate variations, we employ the method of "variation partitioning" (Peres-Neto et al., 2006). We have fitted three basis functions to the 2003-2016 growth rate time series via linear least-squares minimization (we explain the method in this paragraph using SOI but the method does not depend on which ENSO index is used): (i) a constant offset (variance zero), (ii) the human CO_2 emissions (Fig. 5b) and (iii) SOI shifted by 7 months (blue solid line in Fig. 5d). The variance of the scaled emission, i.e., of the human emission scaled with the corresponding fit parameter, is 0.0758 $ppm^2/year^2$ (note that in this section we report numerical values with four digital places but this shall not imply that all decimal places are significant). The variance of the scaled SOI is 0.1070 $ppm^2/year^2$ and the variance of the fit residual is 0.0728 $ppm^2/year^2$. The sum of the three individual variances is 0.2557 $ppm^2/year^2$ whereas the variance of the annual mean growth rate is 0.2307 $ppm^2/year^2$. This shows that the sum of the variances is 10.8% larger than the variance of the growth rate, i.e., the sum of the variances is not exactly equal to the variance of the sum. The reason for this is that the CO_2 emission and the SOI time series are not uncorrelated (R = 0.14). To account for correlations, we subtract the variance of the residual from the variance of the growth rate. The result is the part of the variance to be explained by the emissions and by the SOI. The ratio of this to be explained variance (0.1579 $ppm^2/year^2$) and the sum of the variances of the emissions and SOI ((0.0758 + 0.1070) $ppm^2/year^2$ = 0.1828 $ppm^2/year^2$) is 0.8638. The latter is then used as a scaling factor applied to the variances of the emissions and of the SOI. The scaled variances are 0.0655 $ppm^2/year^2$ for the emissions and 0.0924 $ppm^2/year^2$ for SOI (note that the sum of these scaled variances and the variance of the residual is equal to the variance of the growth rate). From this we conclude that the human emissions explain 28% (= 0.0655/0.2307) of the variance of the growth rate and that ENSO as quantified by the SOI explains 40% (= 0.0924/0.2307). We computed (1-sigma) uncertainties of these estimates by numerically perturbing the satellite-derived annual mean growth rates taking into account their uncertainty (see Fig. 4) and by subsequently repeating the computations as explained above 10,000 times. The perturbations correspond to random perturbations of the annual mean growth rates assuming normal distributions for each year and no correlation between the different years. This analysis yields that 40±13% of the growth rate variation results from the impact of ENSO and that 28±14% is due to the human emissions of CO_2. Using these simulations, we also computed the fraction of cases where the ENSO impact dominates over the human emissions. This fraction is

Gelöscht: 2
Gelöscht: 7
Gelöscht: for both cases
Gelöscht: 43
Gelöscht: 128
Gelöscht: 40
Gelöscht: 611
Gelöscht: 5
Gelöscht: -
Gelöscht: 617
Gelöscht: 43
Gelöscht: 128
Gelöscht: 71
Gelöscht: 45
Gelöscht: 42
Gelöscht: 75
Gelöscht: 7
Gelöscht: 42
Gelöscht: 5
Gelöscht: 1
Gelöscht: 75
Gelöscht: 5
Gelöscht: 1
Gelöscht: 7

63% in this case, i.e., when using SOI and when the analysis is applied to the entire time period 2003-2016. This fraction is interpreted as the probability that ENSO-induced impacts on the variation of the growth rate dominates that of human emissions.

When using ONI instead of SOI, ENSO explains 37±14% of the growth rate variance during 2003-2016, human emissions explain 24±14% and the fraction where ENSO dominates is again 63%. When restricting the time period to 2010-2016, which is dominated by strong 2010/2012 La Niña events (Boening et al., 2012; Rodrigues et al., 2014) and by the strong 2015/2016 El Niño, the results are the following: Using the SOI analysis, we find that ENSO explains 58±19% of the variance, human emissions explain 2±9% and the probability that ENSO dominates is 94%. For the ONI analysis, we find that ENSO explains 59±20% of the variance, human emissions explain 3±9% and the probability that ENSO dominates is 94%. This analysis shows that the ENSO impact on CO_2 growth rate variations dominates over that of human emissions throughout the period 2003-2016 but in particular in the second half of this period, i.e., during 2010-2016.

Gelöscht: 6
Gelöscht: 8
Gelöscht: 2
Gelöscht: 3
Gelöscht: 6
Gelöscht: 9
Gelöscht: 1
Gelöscht: 8
Gelöscht: 5
Gelöscht: 2
Gelöscht: 8

5 Conclusions

We presented a method for the computation of atmospheric CO_2 column annual mean growth rates from satellite XCO_2 retrievals. The satellite XCO_2 data product used is the Obs4MIPs version 3 (O4Mv3) XCO_2 data product based on SCIAMACHY/ENVISAT and TANSO-FTS/GOSAT satellite data. This product covers the time period 2003-2016 and has monthly time and 5^ox5^o spatial resolution.

The presented method has been applied to the global satellite data and to selected latitude bands. The estimated uncertainty of the satellite-derived annual mean growth rates is typically in the range 0.3-0.5 ppm/year (1-sigma). The global growth rates agree with NOAA within the uncertainty of the satellite-derived growth rates (mean difference ± standard deviation: 0.0±0.3 ppm/year; R: 0.82). In agreement with NOAA, we find that the growth rates are largest in the years 2015 and 2016. These growth rates are around 3 ppm/year and are attributed to the 2015/2016 El Niño resulting in large CO_2 emissions from fires and enhanced net biospheric respiration in the tropics relative to normal conditions (Heymann et al., 2017; Liu et al., 2017). Our analysis also shows that the ENSO impact on CO_2 growth rate variations dominates over that of human emissions throughout the period 2003-2016 (14 years) but in particular during the period 2010-2016 (second half of the investigated time period) due to strong La Niña and El Niño events. We estimate the probability that the impact of ENSO on the variability is larger than the impact of human emissions to be 63% for the time period 2003-2016. If the time period is restricted to 2010-2016 this probability increases to 94%.

Gelöscht: 24
Gelöscht: 7
Gelöscht: 6
Gelöscht: -95

In the future, we plan to regularly update the satellite-derived XCO_2 growth rates to monitor this important quantity. This will also include satellite XCO_2 retrievals from other satellite instruments such as XCO_2 from NASA's OCO-2 mission (e.g., Eldering et al., 2017; Reuter et al., 2017c, 2017d).

References

Ballantyne, A. P., Alden, C. B., Miller, J. B., Tans, P. P., and White, J. W. C.: Increase in observed net carbon dioxide uptake by land and oceans during the last 50 years, Nature 488, 70–72, 2012.

Basu, S., Guerlet, S., Butz, A., Houweling, S., Hasekamp, O., Aben, I., Krummel, P., Steele, P., Langenfelds, R., Torn, M., Biraud, S., Stephens, B., Andrews, A., and Worthy, D.: Global CO_2 fluxes estimated from GOSAT retrievals of total column CO_2, Atmos. Chem. Phys., 13, 8695–8717, doi:10.5194/acp-13-8695-2013, 2013.

Boening, C., Willis, J. K., Landerer, F. W., Nerem, R. S., and J. Fasullo, J.: The 2011 La Niña: So strong, the oceans fell, Geophys. Res. Lett., 38, pp. 5, doi:10.1029/2012GL053055, 2012.

Bovensmann, H., Burrows, J. P., Buchwitz, M., Frerick, J., Noël, S., Rozanov, V. V., Chance, K. V., and Goede, A. H. P.: SCIAMACHY - Mission objectives and measurement modes, J. Atmos. Sci., 56 (2), 127-150, 1999.

Buchwitz, M., de Beek, R., Noël, S., Burrows, J. P., Bovensmann, H., Schneising, O., Khlystova, I., Bruns, M., Bremer, H., Bergamaschi, P., Körner, S., and Heimann, M.: Atmospheric carbon gases retrieved from SCIAMACHY by WFM-DOAS: version 0.5 CO and CH_4 and impact of calibration improvements on CO_2 retrieval, Atmos. Chem. Phys., 6, 2727–2751, 2006.

Buchwitz, M., Schneising, O., Burrows, J. P., Bovensmann, H., Reuter, M., and Notholt, J.: First direct observation of the atmospheric CO_2 year-to-year increase from space, Atmos. Chem. Phys., 7, 4249-4256, 2007.

Buchwitz, M., Reuter, M., Schneising, O., Boesch, H., Guerlet, S., Dils, B., Aben, I., Armante, R., Bergamaschi, P., Blumenstock, T., Bovensmann, H., Brunner, D., Buchmann, B., Burrows, J. P., Butz, A., Chédin, A., Chevallier, F., Crevoisier, C. D., Deutscher, N. M., Frankenberg, C., Hase, F., Hasekamp, O. P., Heymann, J., Kaminski, T., Laeng, A., Lichtenberg, G., De Mazière, M., Noël, S., Notholt, J., Orphal, J., Popp, C., Parker, R., Scholze, M., Sussmann, R., Stiller, G. P., Warneke, T., Zehner, C., Bril, A., Crisp, D., Griffith, D. W. T., Kuze, A., O'Dell, C., Oshchepkov, S., Sherlock, V., Suto, H., Wennberg, P., Wunch, D., Yokota, T., and Yoshida, Y.: The Greenhouse Gas Climate Change Initiative (GHG-CCI): comparison and quality assessment of near-surface-sensitive satellite-derived CO_2 and CH_4 global data sets, Remote Sensing of Environment, 162, 344-362, doi:10.1016/j.rse.2013.04.024, 2015.

Buchwitz, M., Reuter, M., Schneising-Weigel, O., Aben, I., Detmers, R. G., Hasekamp, O. P., Boesch, H., Anand,, J., Crevoisier, C., and Armante, R.: Product User Guide and Specification (PUGS) – Main document, Technical Report Copernicus Climate Change Service (C3S), available from C3S website (https://climate.copernicus.eu/) and from http://www.iup.uni-bremen.de/sciamachy/NIR_NADIR_WFM_DOAS/C3S_docs/C3S_D312a_Lot6.3.1.5-v1_PUGS_MAIN_v1.3.pdf, 20/10/2017, pp. 91, 2017a.

Buchwitz, M., Reuter, M., Schneising, O., Hewson, W., Detmers, R. G., Boesch, H., Hasekamp, O. P., Aben, I., Bovensmann, H., Burrows, J. P., Butz, A., Chevallier, F., Dils, B., Frankenberg, C., Heymann, J., Lichtenberg, G., De Mazière, M., Notholt, J., Parker, R., Warneke, T., Zehner, C., Griffith, D. W. T., Deutscher, N. M., Kuze, A., Suto, H., and Wunch, D.: Global satellite observations of column-averaged carbon dioxide and methane: The

GHG-CCI XCO_2 and XCH_4 CRDP3 data set, Remote Sensing of Environment, 203, 276-295, http://dx.doi.org/10.1016/j.rse.2016.12.027, 2017b.

Buchwitz, M., Reuter, M., Schneising-Weigel, O., Aben, I., Detmers, R. G., Hasekamp, O. P., Boesch, H., Anand,, J., Crevoisier, C., and Armante, R.: Product Quality Assessment Report (PQAR) – Main document, Technical Report Copernicus Climate Change Service (C3S), available from C3S website (https://climate.copernicus.eu/) and from http://www.iup.uni-bremen.de/sciamachy/NIR_NADIR_WFM_DOAS/C3S_docs/C3S_D312a_Lot6.3.1.7-v1_PQAR_MAIN_v1.1.pdf, 20/10/2017, pp. 103, 2017c.

Buchwitz, M., Dils, B., Boesch, H., Brunner, D., Butz, A., Crevoisier, C., Detmers, R., Frankenberg, C., Hasekamp, O., Hewson, W., Laeng, A., Noël, S., Notholt, J., Parker, R., Reuter, M., Schneising, O., Somkuti, P., Sundström, A.-M., De Wachter, E.: ESA Climate Change Initiative (CCI) Product Validation and Intercomparison Report (PVIR) for the Essential Climate Variable (ECV) Greenhouse Gases (GHG) for data set Climate Research Data Package No. 4 (CRDP#4), Technical Report, version 5, 9-Feb-2017, link: http://www.esa-ghg-cci.org/?q=webfm_send/352, pp. 253, 2017d.

Burrows, J. P., Hölzle, E., Goede, A. P. H., Visser, H., and Fricke, W.: SCIAMACHY—Scanning Imaging Absorption Spectrometer for Atmospheric Chartography, Acta Astronaut., 35(7), 445–451, doi:10.1016/0094-5765(94)00278-t, 1995.

Butz, A., Guerlet, S., Hasekamp, O., Schepers, D., Galli, A., Aben, I., Frankenberg, C., Hartmann, J.-M., Tran, H., Kuze, A., Keppel-Aleks, G., Toon, G., Wunch, D., Wennberg, P., Deutscher, N., Griffith, D., Macatangay, R., Messerschmidt, J., Notholt, J., and Warneke, T.: Toward accurate CO_2 and CH_4 observations from GOSAT, Geophys. Res. Lett., doi:10.1029/2011GL047888, 2011.

Chevallier, F., Palmer, P. I., Feng, L., Boesch, H., O'Dell, C. W., and Bousquet, P.: Towards robust and consistent regional CO_2 flux estimates from in situ and space-borne measurements of atmospheric CO_2, Geophys. Res. Lett., 41, 1065–1070, doi:10.1002/2013GL058772, 2014.

Chylek, P., Tans, P., Christy, P., and Dubey, M. K.: The carbon cycle response to two El Nino types: an observational study, Environ. Res. Lett., 13, pp. 8, https://doi.org/10.1088/1748-9326/aa9c5b, 2018.

Cogan, A. J., Boesch, H., Parker, R. J., Feng, L., Palmer, P. I., Blavier, J.-F. L., Deutscher, N. M., Macatangay, R., Notholt, J., Roehl, C., Warneke, T., and Wunsch, D.: Atmospheric carbon dioxide retrieved from the Greenhouse gases Observing SATellite (GOSAT): Comparison with ground-based TCCON observations and GEOS-Chem model calculations, J. Geophys. Res., 117, D21301, doi:10.1029/2012JD018087, 2012.

Dlugokencky, E., and Tans, P.: Trends in atmospheric carbon dioxide. National Oceanic & Atmospheric Administration, Earth System Research Laboratory (NOAA/ESRL), 2017a.

Dlugokencky, E., and Tans, P.: Trends in atmospheric carbon dioxide, National Oceanic & Atmospheric Administration, Earth System Research Laboratory (NOAA/ESRL), file: ftp://aftp.cmdl.noaa.gov/products/trends/co2/co2_gr_gl.txt (access: 24 November 2017), 2017b.

Eldering, A. et al. The Orbiting Carbon Observatory-2: first 18 months of science data products, Atmos. Meas. Tech., 10, 549-563, https://doi.org/10.5194/amt-10-549-2017, 2017.

GCP: Global CO_2 emissions from Global Carbon Project (GCP) website (http://www.globalcarbonproject.org/carbonbudget/17/data.htm), main data source: Thomas Boden, Gregg Marland, Robert Andres 2017 (CDIAC), GCP-CICERO, UNFCCC, BP Statistical Review of World Energy (BP, 2017), US Geological Survey (USGS, 2017), 2017.

Hakkarainen, J., Ialongo, I., and Tamminen, J.: Direct space-based observations of anthropogenic CO_2 emission areas from OCO-2, Geophys. Res. Lett., 43, 11,400–11,406, doi:10.1002/2016GL070885, 2016.

Heymann, J., Reuter, M., Buchwitz, M., Schneising, O., Bovensmann, H., Burrows, J. P., Massart, S., Kaiser, J. W., and Crisp, D.: CO_2 emission of Indonesian fires in 2015 estimated from satellite-derived atmospheric CO_2 concentrations, Geophys. Res. Lett., doi:10.1002/2016GL072042, pp. 18, 2017.

Houweling, S., Baker, D., Basu, S., Boesch, H., Butz, A., Chevallier, F., Deng, F., Dlugokencky, E. J., Feng, L., Ganshin, A., Hasekamp, O., Jones, D., Maksyutov, S., Marshall, J., Oda, T., O'Dell, C. W., Oshchepkov, S., Palmer, P. I., Peylin, P., Poussi, Z., Reum, F., Takagi, H., Yoshida, Y., and Zhuralev, R.: An intercomparison of inverse models for estimating sources and sinks of CO_2 using GOSAT measurements, J. Geophys. Res. Atmos., 120, 5253–5266, doi:10.1002/2014JD022962, 2015.

Huntzinger, D. N., Michalak, A. M., Schwalm, C., Ciais, P., King, A. W., Fang, Y., Schaefer, K., Wei, Y., Cook, R. B., Fisher, J. B., Hayes, D., Huang, M., Ito, A., Jain, A. K., Lei, H., Lu, C., Maignan, F., Mao, J., Parazoo, N., Peng, S., Poulter, B., Ricciuto, D., Shi, X., Tian, H., Wang, W., Zeng, N., and Zhao, F.: Uncertainty in the response of terrestrial carbon sink to environmental drivers undermines carbon-climate feedback predictions, Nature, Scientific Reports, 7: 4765, doi:10.1038/s41598-017-03818-2, 2017.

IPCC: Climate Change 2013: The Physical Science Basis, Working Group I Contribution to the Fifth Assessment Report of the Intergovernmental Report on Climate Change, http://www.ipcc.ch/report/ar5/wg1/, Cambridge University Press, 2013.

Jones, C. D., Collins, M., Cox, P. M., and Spall, S. A.: The Carbon Cycle Response to ENSO: A Coupled Climate-Carbon Cycle Model Study, Journal of Climate, Vol. 14, 4113-4129, 2001.

Kaminski, T., Scholze, M., Voßbeck, M., Knorr, W., Buchwitz, M, and Reuter, M.: Constraining a terrestrial biosphere model with remotely sensed atmospheric carbon dioxide, Remote Sensing of Environment 203, 109-124, 2017.

Kort, E., Frankenberg, C., Miller, C. E., and Oda, T.: Space-based observations of megacity carbon dioxide. Geophys. Res. Lett., 39, doi:10.1029/2012GL052738, 2012.

Kuze, A., Suto, H., Shiomi, K., Kawakami, S., Tanaka, M., Ueda, Y., Deguchi, A., Yoshida, J., Yamamoto, Y., Kataoka, F., Taylor, T. E., and Buijs, H. L.: Update on GOSAT TANSO-FTS performance, operations, and data products after more than 6 years in space, Atmos. Meas. Tech., 9, 2445-2461, doi:10.5194/amt-9-2445-2016, 2016.

Lauer, A., Eyring, V., Righi, M., Buchwitz, M., Defourny, P., Evaldsson, M., Friedlingstein, P., de Jeu, R., de Leeuw, G., Loew, A., Merchant, C. J., Müller, B., Popp, T., Reuter, M., Sandven, S., Senftleben, D., Stengel, M., Van Roozendael, M., Wenzel, S., and Willén, U.: Benchmarking CMIP5 models with a subset of ESA CCI Phase 2 data using the ESMValTool, Remote Sensing of Environment, 203, 9-39, http://dx.doi.org/10.1016/j.rse.2017.01.007, 2017.

Le Quéré, C., Andrew, R. M., Canadell, J. G., Sitch, S., Korsbakken, J. I., Peters, G. P., Manning, A. C., Boden, T. A., Tans, P. P., Houghton, R. A., Keeling, R. F., Alin, S., Andrews, O. D., Anthoni, P., Barbero, L., Bopp, L., Chevallier, F., Chini, L. P., Ciais, P., Currie, K., Delire, C., Doney, S. C., Friedlingstein, P., Gkritzalis, T., Harris, I., Hauck, J., Haverd, V., Hoppema, M., Klein Goldewijk, K., Jain, A. K., Kato, E., Körtzinger, A., Landschützer, P., Lefèvre, N., Lenton, A., Lienert, S., Lombardozzi, D., Melton, J. R., Metzl, N., Millero, F., Monteiro, P. M. S., Munro, D. R., Nabel, J. E. M. S., Nakaoka, S. I., O'Brien, K., Olsen, A., Omar, A. M., Ono, T., Pierrot, D., Poulter, B., Rödenbeck, C., Salisbury, J., Schuster, U., Schwinger, J., Séférian, R., Skjelvan, I., Stocker, B. D., Sutton, A. J., Takahashi, T., Tian, H., Tilbrook, B., van der Laan-Luijkx, I. T., van der Werf, G. R., Viovy, N., Walker, A. P., Wiltshire, A. J., and Zaehle, S.: Global Carbon Budget 2016, Earth Syst. Sci. Data, 8, 605-649, 2016.

Le Quéré, C., Andrew, R. M., Friedlingstein, P., Sitch, S., Pongratz, J., Manning, A. C., Korsbakken, J. I., Peters, G. P. Canadell, J. G., Jackson, R. B., Boden, T. A., Tans, P. P., Andrews, O. D., Arora, V. K., Bakker, D. D. E, Barbero, L., Becker, M., Betts, R. A., Bopp, L., Chevallier, F., Chini, L. P., Ciais, P., Cosca, C. E., Cross, J., Currie, K., Gasser, T., Harris, I., Hauck, J., Haverd, V., Houghton, R. A., Hunt, C. W., Hurtt, G., Ilyina, T., Jain, A. K., Kato, E., Kautz, M., Keeling, R. F., Goldewijk, K. K., Körtzinger, A., Landschützer, P., Lefèvre, N., Lenton, A., Lienert, S., Lima, I., Lombardozzi, D., Metzl, N., Millero, F., Monteiro, P. M. S., Munro, D. R., Nabel, J. E. M. S., Nakaoka, S., Nojiri, Y., Padín, X. A., Peregon, A., Pfeil, B., Pierrot, D., Poulter, B., Rehder, G., Reimer, J., Rödenbeck, C., Schwinger, J., Séférian, R., Skjelvan, I., Stocker, B. D., Tian, H., Tilbrook, B., van der Laan-Luijkx, I. T., van der Werf, G. R., van Heuven, S., Viovy, N., Vuichard, N., Walker, A. P., Watson, A. J., Wiltshire, A. J., Zaehle, S., and Zhu, D.: Global Carbon Budget 2017, Earth System Science Data, 10, 405-448, DOI: 10.5194/essd-10-405-2018, 2018.

Liu, J., Bowman, K. W., Schimel, D. S., Parazoo, N. C., Jiang, Z., Lee, M., Bloom, A. A., Wunch, D., Frankenberg, C., Sun, Y., O'Dell, C. W., Gurney, K. R., Menemenlis, D., Gierach, M., Crisp, D., and Eldering, A.: Contrasting carbon cycle responses of the tropical continents to the 2015–2016 El Niño, Science, 358, eaam5690, pp. 7, 2017.

Maksyutov, S., Takagi, H., Valsala, V. K., Saito, M., Oda, T., Saeki, T., Belikov, D. A., Saito, R., Ito, A., Yoshida, Y., Morino, I., Uchino, O., Andres, R. J., and Yokota, T.: Regional CO_2 flux estimates for 2009–2010 based on GOSAT and ground-based CO_2 observations, Atmos. Chem. Phys., 13, 9351-9373, 2013.

Nassar, R., Hill, T. G., McLinden, C. A., Wunch, D., Jones, D. B. A., and Crisp, D.: Quantifying CO_2 emissions from individual power plants from space, Geophys. Res. Lett., doi:10.1002/2017GL074702, 2017.

NIES: Recent global CO_2 (http://www.gosat.nies.go.jp/en/recent-global-co2.html), 2017.

Gelöscht: Discussions

Gelöscht: d

Gelöscht: 7-123

Gelöscht: 7

NOAA: Southern Oscillation Index (SOI), file https://www.esrl.noaa.gov/psd/gcos_wgsp/Timeseries/Data/soi.long.data, data based on the method of Ropelewski and Jones, 1987, using data from the Climate Research Unit (CRU; http://www.cru.uea.ac.uk/cru/data/soi/), 2017a.

NOAA: Oceanic Niño Index (ONI), file https://www.esrl.noaa.gov/psd/data/correlation/oni.data obtained from https://www.esrl.noaa.gov/psd/data/climateindices/list, 2017b.

O'Dell, C. W., Connor, B., Bösch, H., O'Brien, D., Frankenberg, C., Castano, R., Christi, M., Eldering, D., Fisher, B., Gunson, M., McDuffie, J., Miller, C. E., Natraj, V., Oyafuso, F., Polonsky, I., Smyth, M., Taylor, T., Toon, G. C.,Wennberg, P. O., andWunch, D.: The ACOS CO_2 retrieval algorithm – Part 1: The ACOS CO_2 retrieval algorithm – Part 1: Description and validation against synthetic observations, Atmos. Meas. Tech., 5, 99–121, doi:10.5194/amt-5-99-2012, 2012.

Parker, R. J., Boesch, H., Wooster, M. J., Moore, D. P., Webb, A. J., Gaveau, D., and Murdiyarso, D.: Atmospheric CH_4 and CO_2 enhancements and biomass burning emission ratios derived from satellite observations of the 2015 Indonesian fire plumes, Atmos. Chem. Phys., 16, 10111-10131, doi:10.5194/acp-16-10111-2016, 2016.

Peres-Neto, P. R., Legendre, P., Dray, S., and Borcard, D.: Variation partitioning of species data matrices: Estimation and comparison of fractions, Ecology, 87(19), pp. 2614-2625, 2006.

Peters, W., Jacobson, A. R., Sweeney, C., Andrews, A. E., Conway, T. J., Masarie, K., Miller, J. B., Bruhwiler, L. M. P., Pétron, G., Hirsch, A. I., Worthy, D. E. J., van der Werf, G. R., Randerson, J. T., Wennberg, P. O., Krol, M. C., and Tans, P. P.: An atmospheric perspective on North American carbon dioxide exchange: CarbonTracker, Proc. Natl. Acad. Sci. USA, 104, 18925–18930, doi:10.1073/pnas.0708986104, 2007.

Peters, G. P., Le Quéré, C., Andrew, R. M., Canadell, J. G., Friedlingstein, P., Ilyina, T., Jackson, R., Joos, F., Korsbakken, J. I., McKinley, G. A., Sitch, S., and Tans, P.: Towards real-time verification of CO_2 emissions, Nature Climate Change, 13 November 2017, doi:10.1038/s41558-017-0013-9, 2017.

Peylin, P., Law, R. M., Gurney, K. R., Chevallier, F., Jacobson, A. R., Maki, T., Niwa, Y., Patra, P. K., Peters, W., Rayner, P. J., Rödenbeck, C., van der Laan-Luijkx, I. T., and Zhang, X.: Global atmospheric carbon budget: results from an ensemble of atmospheric CO_2 inversions, Biogeosciences, 10, 6699–6720, doi:10.5194/bg-10-6699-2013, 2013.

Reuter, M., Bovensmann, H., Buchwitz, M., Burrows, J. P., Connor, B. J., Deutscher, N. M., Griffith, D. W. T., Heymann, J., Keppel-Aleks, G., Messerschmidt, J., Notholt, J., Petri, C., Robinson, J., Schneising, O., Sherlock, V., Velazco, V., Warneke, W., Wennberg, P. O., and Wunch, D.: Retrieval of atmospheric CO_2 with enhanced accuracy and precision from SCIAMACHY: Validation with FTS measurements and comparison with model results, J. Geophys. Res., 116, D04301, doi:10.1029/2010JD015047, 2011.

Reuter, M., H. Boesch, H. Bovensmann, A. Bril, M. Buchwitz, A. Butz, J. P. Burrows, C. W. O'Dell, S. Guerlet, O. Hasekamp, J. Heymann, N. Kikuchi, S. Oshchepkov, R. Parker, S. Pfeifer, O. Schneising, T. Yokota, and Y.

Gelöscht: Prather, M. J., Holmes, C. D., and Hsu, J.: Reactive greenhouse gas scenarios: Systematic exploration of uncertainties and the role of atmospheric chemistry, Geophys. Res. Lett., 39, L09803, doi:10.1029/2012GL051440, 2012. ¶

Yoshida: A joint effort to deliver satellite retrieved atmospheric CO_2 concentrations for surface flux inversions: the ensemble median algorithm EMMA, Atmos. Chem. Phys., 13, 1771-1780, 2013.

Reuter, M., Buchwitz, M., Hilker, M., Heymann, J., Schneising, O., Pillai, D., Bovensmann, H., Burrows, J. P., Bösch, H., Parker, R., Butz, A., Hasekamp, O., O'Dell, C. W., Yoshida, Y., Gerbig, C., Nehrkorn, T., Deutscher, N. M., Warneke, T., Notholt, J., Hase, F., Kivi, R., Sussmann, R., Machida, T., Matsueda, H., and Sawa, Y.: Satellite-inferred European carbon sink larger than expected, Atmos. Chem. Phys., 14, 13739-13753, 2014a.

Reuter, M., Buchwitz, M., Hilboll, A., Richter, A., Schneising, O., Hilker, M., Heymann, J., Bovensmann, H., and Burrows, J. P.: Decreasing emissions of NOx relative to CO_2 in East Asia inferred from satellite observations, Nature Geoscience, 28 Sept. 2014, doi:10.1038/ngeo2257, pp. 4, 2014b.

Reuter, M., Buchwitz, M., Schneising, O., Noël, S., Rozanov, V., Bovensmann, H., and Burrows, J. P.: A Fast Atmospheric Trace Gas Retrieval for Hyperspectral Instruments Approximating Multiple Scattering - Part 1: Radiative Transfer and a Potential OCO-2 XCO_2 Retrieval Setup, Remote Sens., 9, 1159, doi:10.3390/rs9111159, 2017c.

Reuter, M., Buchwitz, M., Schneising, O., Noël, S., Bovensmann, H., and Burrows, J. P.: A Fast Atmospheric Trace Gas Retrieval for Hyperspectral Instruments Approximating Multiple Scattering - Part 2: Application to XCO_2 Retrievals from OCO-2, Remote Sens., 9, 1102, doi:10.3390/rs9111102, 2017d.

Reuter, M., Buchwitz, M., and Schneising-Weigel, O.: Algorithm Theoretical Basis Document (ATBD) – ANNEX D for products XCO2_EMMA and XCH4_EMMA. Technical Report Copernicus Climate Change Service (C3S), available from C3S website (https://climate.copernicus.eu/) and from http://www.iup.uni-bremen.de/sciamachy/NIR_NADIR_WFM_DOAS/C3S_docs/C3S_D312a_Lot6.2.1.2-v1_ATBD_ANNEX-D_v1.1.pdf, 20/10/2017, pp. 32, 2017e.

Rodrigues, R. R., and McPhaden, M. J.: Why did the 2011-2012 La Niña cause a severe drought in the Brazilian Northeast? Geophys. Res. Lett., 41, 1012–1018, doi:10.1002/2013GL058703, 2014.

Ropelewski, C. F., and Jones, P. D.: An extension of the Tahiti-Darwin Southern Oscillation Index. Monthly Weather Review, 115, 2161-2165, 1987.

Schneising, O., Heymann, J., Buchwitz, M., Reuter, M., Bovensmann, H., and Burrows, J. P.: Anthropogenic carbon dioxide source areas observed from space: assessment of regional enhancements and trends, Atmos. Chem. Phys., 13, 2445-2454, doi:10.5194/acp-13-2445-2013, 2013.

Schneising, O., Reuter, M., Buchwitz, M., Heymann, J., Bovensmann, H., and Burrows, J. P.: Terrestrial carbon sink observed from space: variation of growth rates and seasonal cycle amplitudes in response to interannual surface temperature variability, Atmos. Chem. Phys., 14, 133-141, 2014.

Thoning, K. W., Tans, P. P., and Komhyr, W. D.: Atmospheric carbon dioxide at Mauna Loa Observatory, 2. Analysis of the NOAA/GMCC data. 1974-1985, J. Geophys. Res., 94, 8549-8565, 1989.

Wieder, W. R., Cleveland, C. C., Smith, W. K., and Todd-Brown, K.: Future productivity and carbon storage limited by terrestrial nutrient availability, Nature Geoscience, doi:10.1038/NGEO2313, 2015.

Wunch, D., Toon, G. C., Blavier, J.-F. L., Washenfelder, R. A., Notholt, J., Connor, B. J., Griffith, D. W. T., Sherlock, V., and Wennberg, P. O.: The Total Carbon Column Observing Network. Phil. Trans. R. Soc. A, 369, 2087–2112, doi:10.1098/rsta.2010.0240, 2011.

Wunch, D., Toon, G. C., Sherlock, V., Deutscher, N. M, Liu, X., Feist, D. G., and Wennberg, P. O.: The Total Carbon Column Observing Network's GGG2014 Data Version, Carbon Dioxide Information Analysis Center, Oak Ridge National Laboratory, Oak Ridge, Tennessee, USA, available at: doi:10.14291/tccon.ggg2014.documentation.R0/1221662, 2015.

Yoshida, Y., Kikuchi, N., Morino, I., Uchino, O., Oshchepkov, S., Bril, A., Saeki, T., Schutgens, N., Toon, G. C., Wunch, D., Roehl, C. M., Wennberg, P. O., Griffith, D. W. T, Deutscher, N. M., Warneke, T., Notholt, J., Robinson, J., Sherlock, V., Connor, B., Rettinger, M., Sussmann, R., Ahonen, P., Heikkinen, P., Kyrö, E., Mendonca, J., Strong, K., Hase, F., Dohe, S., and Yokota, T.: Improvement of the retrieval algorithm for GOSAT SWIR XCO_2 and XCH_4 and their validation using TCCON data, Atmos. Meas. Tech., 6, 1533–1547, doi:10.5194/amt-6-1533-2013, 2013.

Acknowledgements

This study has been funded in parts by the European Space Agency (ESA) (via the GHG-CCI project of ESA's Climate Change Initiative (CCI, http://www.esa-ghg-cci.org/)), by the European Union (EU) (via the Copernicus Climate Change Service (C3S, https://climate.copernicus.eu/) managed by the European Centre for Medium-range Weather Forecasts (ECMWF)) and by the State and the University of Bremen. The University of Leicester GOSAT retrievals used the ALICE High Performance Computing Facility at the University of Leicester. We thank ESA/DLR for providing us with SCIAMACHY Level 1 data products and JAXA for GOSAT Level 1B data. We also thank ESA for making these GOSAT products available via the ESA Third Party Mission archive. We thank NIES for the operational GOSAT XCO_2 Level 2 product and the NASA/ACOS team for the GOSAT ACOS Level 2 XCO_2 product. We also thank NOAA for the global CO_2 growth rates (file ftp://aftp.cmdl.noaa.gov/products/trends/co2/co2_gr_gl.txt; access: 24-Nov-2017). The fossil fuel and industry CO_2 emissions have been obtained from the Global Carbon Project website (http://www.globalcarbonproject.org/carbonbudget/17/data.htm; access: 20-Nov-2017). The Southern Oscillation Index (SOI) data have been obtained from NOAA (file https://www.esrl.noaa.gov/psd/gcos_wgsp/Timeseries/Data/soi.long.data; access: 20-Nov-2017). The Oceanic Niño Index (ONI) data have also been obtained from NOAA (file https://www.esrl.noaa.gov/psd/data/correlation/oni.data).

Author contributions

M.B. supported by O.S., M.R., H.Bov., S.N., B.G., J.P.B.: design, data analysis, interpretation and writing of the paper. The paper has been significantly improved by: H.Boe., J.A., R.J.P., P.S., R.G.D., O.P.H., I.A., A.B., A.K., H.S., Y.Y., D.C., C.O'D. Satellite input data have been provided by: M.R., M.B., O.S. (SCIAMACHY products) and H.Boe., J.A., R.J.P., P.S., R.G.D., O.P.H., I.A., A.B., A.K., H.S., Y.Y., D. C., C.O'D. (GOSAT products).

Data availability. The O4Mv3 XCO_2 data product (but also the underlying EMMAv3 product and those individual sensor Level 2 input products which have been generated with European retrieval algorithms) will be available (around June 2018) via the Copernicus Climate Change Service (C3S, https://climate.copernicus.eu/) Climate Data Store (CDS). Earlier versions are available from the GHG-CCI website (http://www.esa-ghg-cci.org/) of the European Space Agency (ESA) Climate Change Initiative (CCI, e.g., Obs4MIPs version 2 (O4Mv2) covering the years 2003-2015).

Gelöscht: in

Gelöscht: April/May

Competing financial interests

The authors declare no competing financial interests.

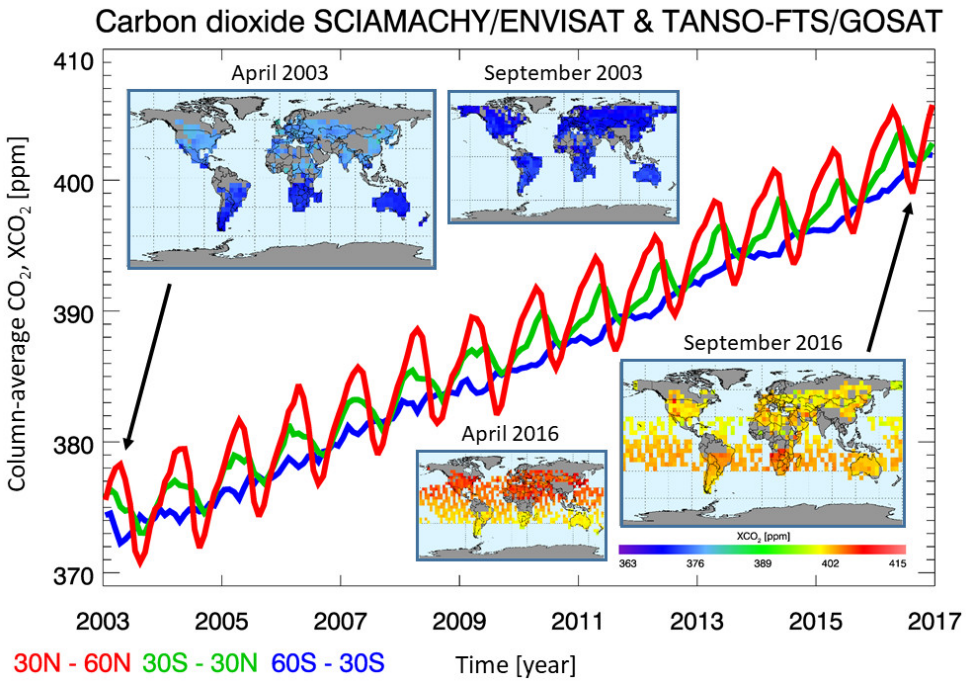

Figure 1. Time series and global maps of satellite-derived column-average dry-air mole fractions of carbon dioxide, i.e., XCO_2. Shown is data product Obs4MIPs version 3 (O4Mv3) based on an ensemble of SCIAMACHY/ENVISAT (until April 2012) and TANSO-FTS/GOSAT (since mid 2009) individual sensor / individual soundings (Level 2) data products. The three time series correspond to three latitude bands: 30°N-60°N (red), 30°S-30°N (green) and 60°S-30°S (blue). The maps in the top left show monthly XCO_2 for April and September 2003 (SCIAMACHY, land only) and the maps on the bottom right show monthly XCO_2 for April and September 2016 (TANSO-FTS, land and ocean glint).

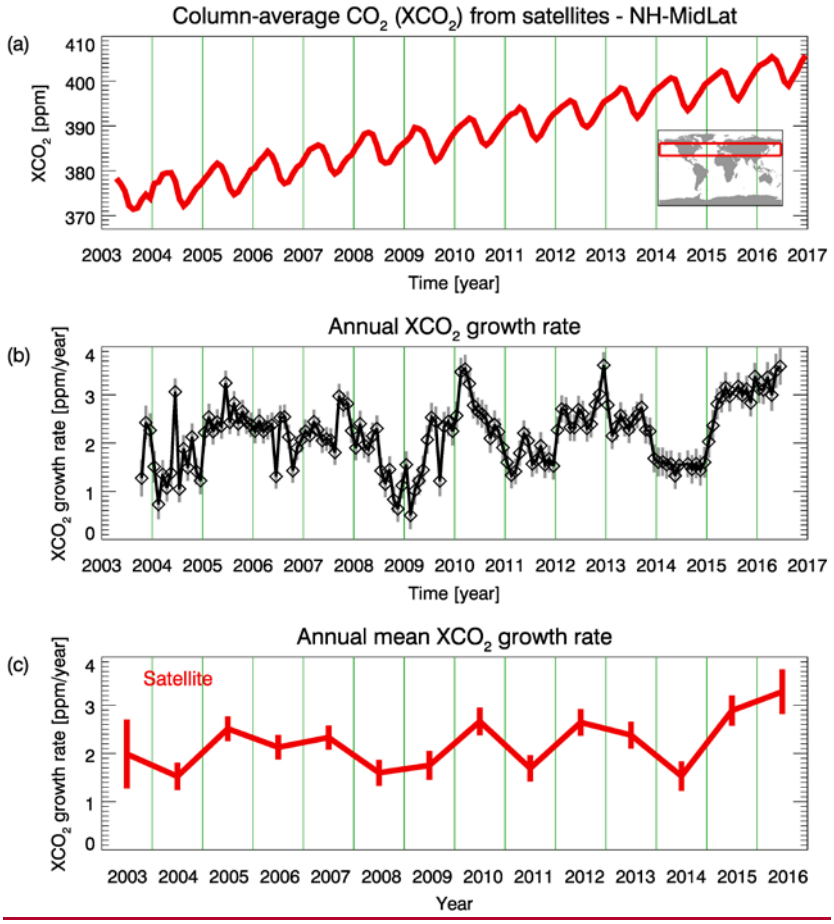

Figure 2. Atmospheric CO_2 and corresponding growth rates for northern mid-latitudes. (a) Monthly mean XCO_2 (red line) for northern mid-latitudes obtained from averaging XCO_2 data product O4Mv3 in the latitude band 30°N-60°N (see red rectangle in global map). (b) Monthly sampled annual CO_2 growth rates as computed from the red curve shown in (a) including 1-sigma uncertainty (grey vertical bars). (c) Annual mean growth rates computed from averaging the values shown in (b) including 1-sigma error estimates (vertical bars) (the numerical values are listed in Tab. 2).

Gelöscht:

Formatiert: Zentriert

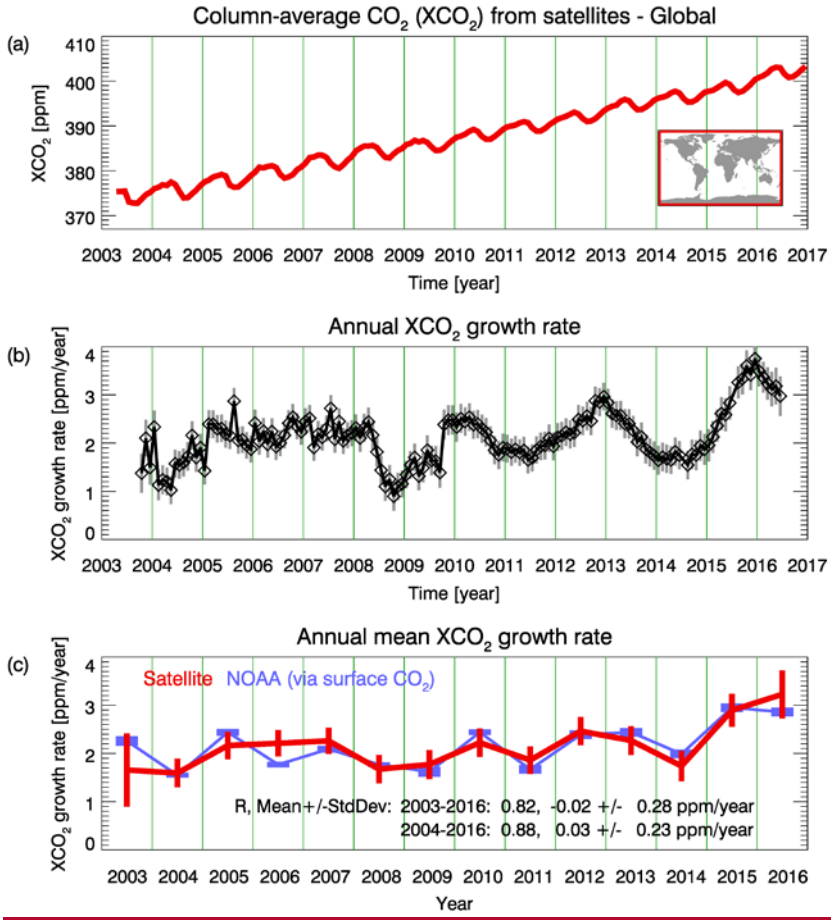

Figure 3. As Fig. 2 but for the entire globe. The NOAA annual mean global growth rate is also shown in **c** for comparison (in blue). Also listed in (c) is the linear correlation coefficient (R), the mean difference and the standard deviation of the difference of the satellite and the NOAA growth rates for 2003-2016 and for 2004-2016.

Gelöscht:

Formatiert: Zentriert

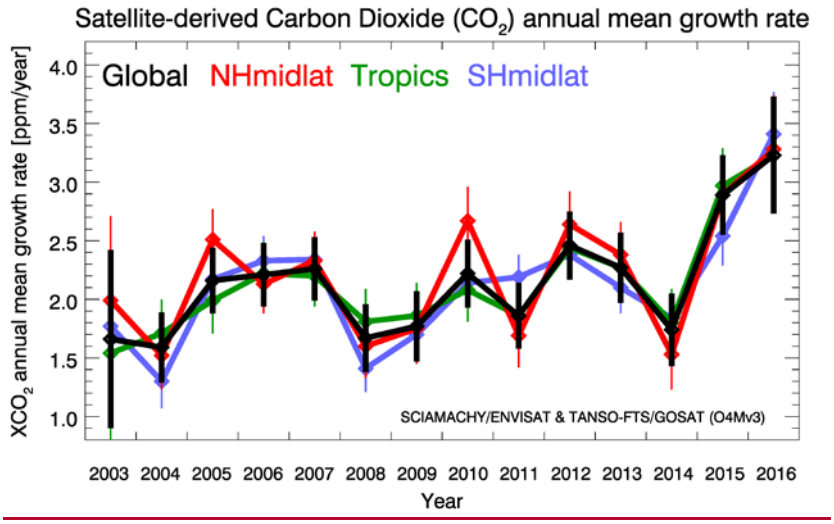

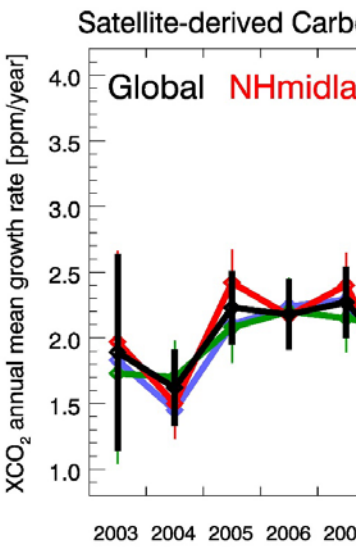

Gelöscht:

Formatiert: Zentriert

Figure 4. Satellite-derived annual mean XCO_2 growth rates: Global (black), Northern Hemisphere (NH) mid latitudes ("NHmidlat" (30°N - 60°N), red), Tropics (30°S - 30°N, green), and Southern Hemisphere mid latitudes ("SHmidlat" (60°S - 30°S), blue). The corresponding numerical values are listed in Tab. 2.

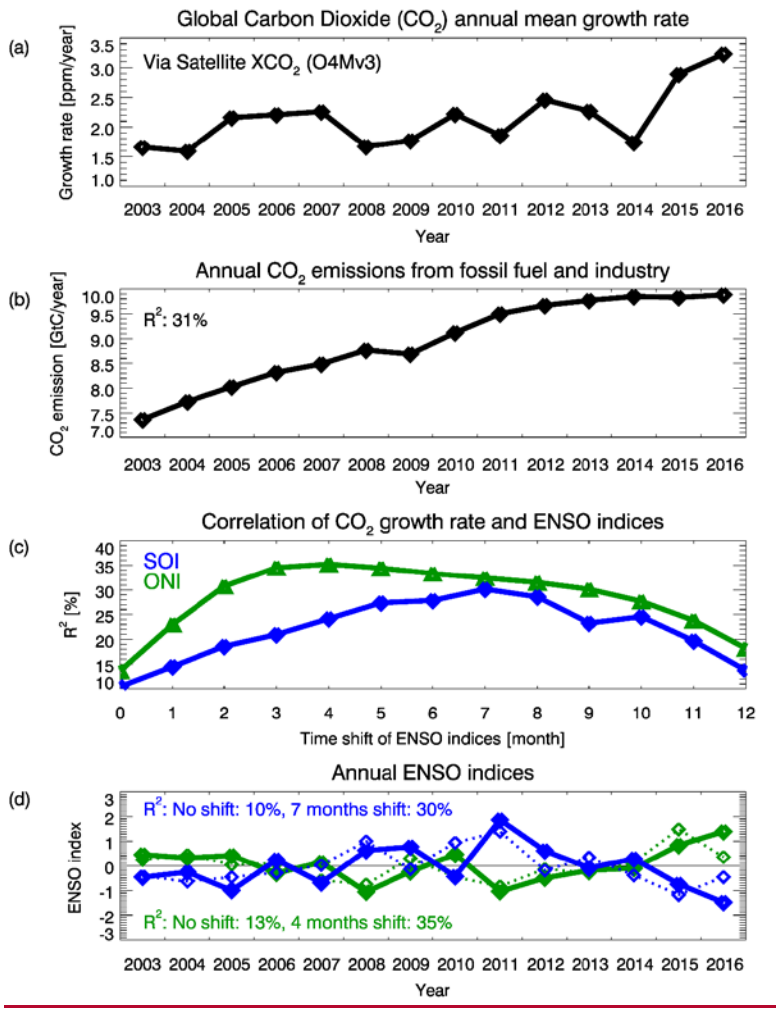

Figure 5. Carbon dioxide global annual mean growth rates compared with human emissions and ENSO indices. (a) Satellite-derived global annual mean growth rates (same as black line in Fig. 4). (b) CO_2 emissions from fossil fuel and industry (the correlation with the growth rate is R^2 = 31%). (c) Correlation in terms of R^2 of growth rate and annual SOI (blue curve) and ONI (green curve) as a function of time shift in months. (d) Annual SOI for no shift (blue dotted line, R^2 = 10%) and for a shift of 7 months (blue solid line, R^2 = 30%) and annual ONI for no shift (green dotted line, R^2 = 13%) and for a shift of 4 months (green solid line, R^2 = 35%).

Gelöscht:

Formatiert: Zentriert

Gelöscht: 2

Gelöscht: 1

Gelöscht: 7

Gelöscht: 2

Gelöscht: 7

Table 1. Satellite XCO_2 data products. Individual satellite sensor XCO_2 algorithms and corresponding Level 2 data products used for generating the EMMAv3 Level 2 (i.e., individual soundings) data product, which has been gridded to obtain the O4Mv3 Level 3 data product used in this study. GHG-CCI refers to the GHG-CCI project of ESA's Climate Change Initiative (http://www.esa-ghg-cci.org/) and C3S is the Copernicus Climate Change Service (https://climate.copernicus.eu/).

Algorithm (Version)	Sensor	Comment	Reference
BESD (v02.01.02)	SCIAMACHY / ENVISAT	GHG-CCI / C3S product ID: CO2_SCI_BESD	Reuter et al., 2011
RemoTeC (v2.3.8)	TANSO-FTS / GOSAT	GHG-CCI / C3S product ID: CO2_GOS_SRFP	Butz et al., 2011
UoL-FP (v7.1)	TANSO-FTS / GOSAT	GHG-CCI / C3S product ID: CO2_GOS_OCFP	Cogan et al., 2012
ACOS (v7.3.10a)	TANSO-FTS / GOSAT	NASA's GOSAT XCO_2 product	O'Dell et al., 2012
NIES (v02)	TANSO-FTS / GOSAT	Operational GOSAT product	Yoshida et al., 2013

Table 2. Satellite-derived annual mean XCO_2 growth rates in ppm/year including 1-sigma uncertainty (in brackets). Abbreviations: NH is Northern Hemisphere and SH is Southern Hemisphere.

Year	Latitude band / region			
	Global	NH mid-latitudes (30°N-60°N)	Tropics (30°S-30°N)	SH mid-latitudes (60°S-30°S)
2003	1.66 (0.76)	1.99 (0.72)	1.54 (0.74)	1.77 (0.62)
2004	1.59 (0.30)	1.52 (0.29)	1.71 (0.29)	1.30 (0.23)
2005	2.16 (0.28)	2.51 (0.26)	1.99 (0.28)	2.17 (0.22)
2006	2.21 (0.27)	2.13 (0.25)	2.22 (0.27)	2.33 (0.21)
2007	2.26 (0.27)	2.33 (0.25)	2.20 (0.26)	2.34 (0.21)
2008	1.67 (0.29)	1.60 (0.27)	1.81 (0.28)	1.41 (0.20)
2009	1.77 (0.30)	1.75 (0.30)	1.86 (0.28)	1.70 (0.21)
2010	2.22 (0.29)	2.67 (0.29)	2.08 (0.27)	2.14 (0.20)
2011	1.86 (0.28)	1.69 (0.27)	1.86 (0.27)	2.19 (0.19)
2012	2.46 (0.29)	2.64 (0.28)	2.44 (0.27)	2.38 (0.21)
2013	2.27 (0.30)	2.38 (0.28)	2.27 (0.28)	2.10 (0.22)
2014	1.74 (0.31)	1.53 (0.30)	1.80 (0.29)	1.84 (0.23)
2015	2.89 (0.34)	2.89 (0.31)	2.97 (0.32)	2.54 (0.25)
2016	3.23 (0.50)	3.28 (0.46)	3.23 (0.48)	3.41 (0.36)

Gelöscht: 89 (0.765
Gelöscht: 7 (0.7269
Gelöscht: 73 (0.7469
Gelöscht: 83 (0.6256
Gelöscht: 62 (0.3029
Gelöscht: 0 (0.297
Gelöscht: 0 (0.298
Gelöscht: 45 (0.231
Gelöscht: 23
Gelöscht: 42 (0.265
Gelöscht: 2.9908…(0.287
Gelöscht: 0 (0.2219
Gelöscht: 18
Gelöscht: 7 (0.254
Gelöscht: 0 (0.276
Gelöscht: 24 (0.2119
Gelöscht: 7
Gelöscht: 40
Gelöscht: 15
Gelöscht: 29 (0.2119
Gelöscht: 79 (0.298
Gelöscht: 56
Gelöscht: 2.8106…(0.286
Gelöscht: 53
Gelöscht: 60 (0.302
Gelöscht: 82
Gelöscht: 68 (0.2830
Gelöscht: 2
Gelöscht: 6 (0.2930
Gelöscht: 6
Gelöscht: 2 (0.2019
Gelöscht: 75 (0.289
Gelöscht: 6
Gelöscht: 78
Gelöscht: 1.19
Gelöscht: 59 (0.2930
Gelöscht: 9
Gelöscht: 51 (0.278
Gelöscht: 52 (0.210
Gelöscht: 5
Gelöscht: 7
Gelöscht: 8
Gelöscht: 5
Gelöscht: 67 (0.312
Gelöscht: 2
Gelöscht: 73
Gelöscht: 79 (0.232
Gelöscht: 8
Gelöscht: 92
Gelöscht: 3
Gelöscht: 60
Gelöscht: 1 (0.5049
Gelöscht: 33
Gelöscht: 19
Gelöscht: 50